
Speciation of dissolved copper within an active hydrothermal edifice on the Lucky Strike vent field (MAR, 37°N)

Pierre-Marie Sarradin^{a,*}, Matthieu Waeles^b, Solène Bernagout^a, Christian Le Gall^a, Jozée Sarrazin^a and Ricardo Riso^b

^a Ifremer centre de Brest, Département Etudes des Ecosystèmes Profonds, BP70, F-29280 Plouzané, France

^b Laboratoire de Chimie Marine, UBO et UMR CNRS 7144, Place Nicolas Copernic, F-29280 Plouzané, France

*: Corresponding author : Pierre-Marie Sarradin' email address : Pierre.Marie.Sarradin@ifremer.fr

Abstract:

The objective of this study was to determine the concentrations of different fractions of dissolved copper (after filtration at 0.45 µm) along the cold part of the hydrothermal fluid-seawater mixing zone on the Tour Eiffel edifice (MAR). Dissolved copper was analyzed by stripping chronopotentiometry (SCP) after chromatographic C18 extraction. Levels of total dissolved copper (0.03 to 5.15 µM) are much higher than those reported for deep-sea oceanic waters but in accordance with data previously obtained in this area. Speciation measurements show that the hydrophobic organic fraction (C18Cu) is very low (2 ± 1%). Dissolved copper is present mainly as inorganic and hydrophilic organic complexes (nonC18Cu). The distribution of copper along the pH gradient shows the same pattern for each fraction. Copper concentrations increase from pH 5.6 to 6.5 and then remain relatively constant at pH > 6.5. Concentrations of oxygen and total sulphides demonstrate that the copper anomaly corresponds to the transition between suboxic and oxic waters. The increase of dissolved copper should correspond to the oxidative redissolution of copper sulphide particles formed in the vicinity of the fluid exit. The presence of such a secondary dissolved copper source, associated with the accumulation of metal sulphide particles, could play a significant role in the distribution of fauna in the different habitats available at vents.

Keywords: Dissolved copper; Speciation; Hydrothermal vent; Mid Atlantic Ridge

34 **1. Introduction**

35

36 The circulation of seawater through fractured rocks at mid oceanic ridges produces important
37 exchanges between lithosphere and hydrosphere. The resulting hydrothermal vents provide
38 hot, reduced and acidic fluids which contain high amounts of various mineral compounds,
39 including hydrogen sulphide, methane, carbon dioxide and many metals such as iron,
40 manganese and copper, (Von Damm et al., 1998; Charlou et al., 2000; Douville et al., 2002).

41 The peculiar and highly productive dense fauna encountered close to hydrothermal vents is
42 not dependant on photosynthesis but rely on microbial chemosynthetic primary producers
43 using reduced chemicals present in the hydrothermal fluid (Childress and Fisher, 1992).

44 Hydrothermal vent fauna is periodically bathed within a variable mixture of hydrothermal
45 fluid and seawater. This environment is chemically highly reactive with the coexistence of
46 oxidized and reduced chemical species (Luther et al., 2001). Steep temperature and chemical
47 gradients are encountered produced by the turbulent mixing of the hot fluid and the cold

48 seawater (Le Bris et al., 2006). The hydrothermal fluid provides to the vent fauna at the same
49 time the necessary energy sources such as methane and hydrogen sulphide (Urcuyo et al.,
50 2003), but also potential stressors or “toxic” compounds such as heavy metals (Douville et al.,

51 2002; Sarradin et al., 2008), high temperature (Shillito et al., in press) or radionuclides. The
52 understanding of the chemical and biological processes controlling the composition of this
53 mixing zone is a necessary step in the study of the functioning of the whole ecosystem

54 (Sarrazin et al., 2006b). The study of trace metals along the hydrothermal fluid-seawater
55 mixing zone is of highly importance because some of these elements and particularly copper
56 can be both essential and toxic for many biological species (Cosson and Vivier, 1997).

57 Mytilids mussels, as well as clams and vestimentiferan tube worms, living in the vent
58 environment accumulate large amounts of metals with surprisingly no evident deleterious

59 effects (Geret et al. 1998, Ruelas-Inzunza et al. 2003 and 2005, Cosson and Vivier 1997,
60 Cosson et al., 2008). To cope with their harmful environment, they have developed efficient
61 mechanisms against the toxicity of heavy metals including their intracellular sequestration as
62 non toxic granules, or the production of metallothioneins and antioxidants (Cosson and
63 Vivier, 1997; Bebianno et al., 2005).

64 Studies exploring the behaviours of metals after their emission in the hydrothermal fluid were
65 mainly focussed on the plume (Trefry and Trocine, 1985; Feely et al., 1990 and 1994; James
66 and Elderfield, 1996). A few authors have started to describe the characteristics of total metal
67 concentrations in the habitats of the hydrothermal fauna (Sarradin et al., 1999; Desbruyères et
68 al., 2001; Geret et al., 2002; Di Meo-Savoie et al., 2004). The main observations arising from
69 these papers presenting concentrations of total metals are the enrichment of this part of the
70 mixing zone accounting for the hydrothermal input and the large variability in the obtained
71 data. However, studies on speciation are necessary to improve our knowledge on metal
72 behaviour and availability in hydrothermal environments. First trials were done on a 2- μ m
73 fractionation for Cu, Zn, Cd and Pb in hydrothermal water samples from the EPR (Sarradin et
74 al., 2008). In particular, the results showed that particulate ($> 2 \mu\text{m}$) and dissolved ($< 2 \mu\text{m}$)
75 Cu were not following a conservative behaviour during the mixing of hydrothermal fluid and
76 seawater.

77 In natural waters, copper coexists under different chemical species such as free hydrated
78 cations $[\text{Cu}(\text{H}_2\text{O})_6]^{2+}$, as well as inorganic complexes (CuOH^+ , $\text{CuCO}_3\dots$) and organic
79 complexes (CuL). Recently, Sander et al. (2007) reported for the first time the important role
80 of organic ligands to control the copper speciation in hydrothermal systems. However, the
81 exact nature and evolution of the various copper species along the hydrothermal fluid-
82 seawater mixing zone are still unknown.

83 The study reported here was carried out in the Tour Eiffel hydrothermal edifice located on the
84 Lucky Strike field on the Mid Atlantic Ridge. Dissolved copper (not retained on a 0.45 μm
85 filter) was analyzed by stripping chronopotentiometry (SCP) after solid-liquid
86 chromatographic C_{18} extraction (Mills and Quinn, 1981). From this extraction, two fractions
87 are obtained: (i) the non-polar hydrophobic organic one (C_{18}Cu) is a subset of the organically-
88 complexed pool and may greatly affect the metal bioavailability (Elbaz-Poulichet et al.,
89 1994); (ii) the second fraction consists of inorganic and hydrophilic organic complexes
90 ($\text{nonC}_{18}\text{Cu}$). It is worth noting that the C_{18} method has been extensively used for studies on
91 estuarine, coastal and oceanic waters (e.g. Mills and Quinn, 1981; Paulson et al., 1994; Elbaz-
92 Poulichet et al., 1994; Yoon et al., 1999; El Sayed and Aminot, 2000; Waeles et al., 2004 and
93 2005) but has never been implemented for hydrothermal systems. Our aim was thus to
94 determine the concentrations of not retained copper and of its various species on an active
95 hydrothermal edifice and also to investigate their changes along the cold part of the
96 hydrothermal fluid-seawater mixing zone.

97

98 **2. Material and methods**

99 *2.1 study area*

100 This study was conducted during the MoMARETO cruise (Sarrazin et al., 2006) held on the
101 French oceanographic vessel “Pourquoi pas?” with the ROV Victor 6000 in 2006. It focussed
102 on the active hydrothermal edifice Tour Eiffel within the Lucky Strike vent field
103 ($37^{\circ}17,29'$ N, $32^{\circ}16,45'$ W) on the Mid Atlantic Ridge (Figure 1). Lucky Strike is one of the
104 largest known active hydrothermal vent fields. The vent sites are distributed around a large
105 lava lake at depths varying from 1650 to 1750 m (Fouquet et al., 1995). Faunal communities
106 are dominated by extensive mussel beds of *Bathymodiolus azoricus* partially covered by
107 visible microbial mats. The vicinity of active high-temperature chimneys, flanges and cracks

108 are colonized by shrimp assemblages (Desbruyères et al., 2001). On the Tour Eiffel edifice, 4
109 or 5 chimneys are venting a hot fluid with a temperature of up to 325°C, concentrations of Fe
110 ranging from 595 to 704 µM and H₂S concentrations of 2100-2500 µM (Charlou et al., 2000).
111 Twelve sampling units were chosen on different sides and at different altitudes on the 11-m
112 tall sulphide edifice in order to have a representative overview of the chemical conditions
113 over the faunal assemblages (Figure 2).

114

115 *2.2 Sampling and sample treatment*

116 Forty two water samples were collected on the 12 sampling units (2-5 samples per station;
117 Figure 2) using the “PEPITO” sampler of the ROV Victor 6000. PEPITO is a new water
118 sampling device qualified up to 6000 m depth (Sarradin et al., 2007). It can collect up to 23
119 water samples in 200 mL titanium/PEEK bottles. All the materials used for the transfer or
120 storage of the samples are chemically inert (PEEK, Titanium, Viton). The manifold is
121 designed to minimize contamination between samples with very low dead volumes. The
122 samples were pumped using a titanium-Tygon inlet associated to the ROV temperature probe.
123 Immediately after the recovery of the ROV, the sampling bottles were carried out to the
124 chemical lab of the oceanographic vessel (clean lab, P 100 000; ISO8). pH measurements
125 were performed on a subsample using a Metrohm® pH-meter with a combined pH electrode
126 (Ingold®) for sulphide rich medium (precision ± 0.01). Measurements were made at 25°C
127 after calibration with NBS buffers (pH 4 and 7). Sample temperatures were derived from the
128 data recorded by the temperature probe associated with the sample inlet. The seawater
129 samples were passed through a 0.45-µm-Millipore®-HATF filter. Dissolved copper in this
130 paper is the operationally (by filter pore size) defined fraction <0.45 µm. A 50-mL aliquot of
131 the filtrate was acidified at pH 2, then stored in Nalgene HDPE bottles at ambient temperature
132 until further analysis of the total dissolved copper (TDCu). Another 100 mL aliquot,

133 maintained at seawater pH, was stored at -20°C in Nalgene HDPE bottles. The separation and
134 the quantification of the hydrophobic organic copper complexes (C₁₈Cu), and the inorganic
135 and hydrophilic organic complexes (nonC₁₈Cu) were performed on shore.

136 Filtrations, C₁₈ extractions and analyses were carried out in class-100 laminar flow hood-
137 equipped laboratories. Prior to use, all the items employed for sampling, filtration and storage
138 were washed several times with diluted hydrochloric acid (pH 2, HCl suprapur®, Merck) and
139 then rinsed with Milli-Q RG® water. The filters were soaked in diluted hydrochloric acid (pH
140 2) for 2 month before the cruise.

141 At each sampling site, in-situ measurements of total sulphide were realized using a new
142 chemical analyzer described in Vuillemin et al. (2007 and submitted). The concentrations of
143 dissolved oxygen and temperature were recorded using an autonomous Optode Aanderaa
144 3830 (Tengberg et al., 2006).

145

146 *2.3 Separation and analyses of the various copper chemical species*

147 Because conventional C₁₈ silica columns are subjected to polar interactions associated with
148 the surface free silanol groups, endcapped C₁₈ columns recently developed by Interchrom®
149 (C₁₈-S-200LRC) for solid-liquid chromatography were selected in order to obtain the non-
150 polar organic fraction with a better accuracy. The protocol used was the one described by
151 Mills and Quinn (1981). The C₁₈ column was first washed by passing successively 10 mL of
152 methanol (G Chromasolv®, Sigma-Aldrich), 10 mL of HCl 3.10⁻² M (Suprapur®, Merck),
153 10 mL of methanol and finally 20 mL of Milli-Q water. Then, 30 mL of the sample were
154 percolated through the column at a flow rate of 10 mL min⁻¹. Elution was achieved by passing
155 6 mL of a methanol/Milli Q water mixture (v/v 1:1). The resulting eluate was completed to
156 30 mL with acidified water at pH 2. The eluted fraction contained the C₁₈Cu species, i.e. the
157 Cu complexed with non polar hydrophobic ligands which includes colloidal Cu (Paulson et

158 al. 1994). The nonC₁₈Cu species were in the unretained fraction and consist of inorganic
159 copper (eg Cu²⁺, CuOH⁻, CuCO₃...) and Cu associated with some non colloidal hydrophilic
160 organic complexes.

161 Recovery tests of the endcapped columns have been conducted on a coastal seawater sample
162 (n=5). The results gave a recovery of 101±12%. 26±5 % of copper was retained on the C₁₈
163 column whereas 75±7% of copper was not retained. Column blanks were prepared by passing
164 100 mL Milli-Q[®] water on the C₁₈ column under the same conditions as for samples. The
165 results obtained for the C₁₈Cu and the nonC₁₈Cu fractions were 0.24 ± 0.16 nM (n = 3) and
166 0.20 ± 0.11 nM (n = 3), respectively. In addition, the concentration of dissolved copper in pH
167 2-acidified Milli-Q[®] water was 0.17 ± 0.10 nM (n = 3). Comparison with this “reference”
168 value showed that the blank ones fell in the same range; thus, no additional contamination
169 was observed from the C₁₈ extraction. Extraction reproducibility was assessed on a coastal
170 seawater sample. Under the same conditions the C₁₈Cu forms account for 26 ± 5% (n = 5) and
171 the nonC₁₈Cu forms account for 75 ± 7% (n = 5).

172 The various copper species (TDCu, C₁₈Cu and nonC₁₈Cu) were measured by stripping
173 chronopotentiometry (SCP) with a gold electrode using the standard method. This method
174 was developed in the lab (Riso et al., 1997a) and has been commonly used in estuarine and
175 coastal waters (Waeles et al., 2004 and 2005). This method is very appropriate for total
176 dissolved copper quantification in organic matter-rich seawater samples since it requires no
177 pretreatment by UV irradiation. The reproducibility is 2% and the detection limit 0.17 nM
178 (Riso et al., 1997a and 1997b). The results obtained for the analysis of copper in certified
179 seawater samples are presented in Table 1.

180

181 **3. Results and discussion**

182 *3.1 Temperature, pH and total dissolved copper*

183 The complete data set is presented in appendix 1. Temperature and pH levels in the 43
184 samples are in the range of 4.6 to 22°C and 5.4 to 7.5 respectively. These values are
185 characteristic of the cold part of the mixing zone between the hydrothermal fluid [T = 324°C,
186 pH 3.5 – 4.2 (Charlou et al., 2000)] and seawater (T = 4.4°C, pH 7.8). The corresponding
187 hydrothermal input can be roughly estimated using the temperature endmember data (Von
188 Damm et al., 1998; Charlou et al., 2000). The calculated fluid input (fluid input % = $0.314T -$
189 1.38) is limited to 0.1 to 5.5%. The possibility of using temperature or pH as dilution tracer of
190 hydrothermal fluid by seawater was tested using the T/pH relationship of our samples. The
191 sigmoid trend obtained (Figure 3) can explain 86% of the variability in the data. This result
192 confirms that at the scale and in the range studied, pH and temperature can be assumed to
193 follow a semi-conservative process and can be used as tracers of the dilution. In this paper,
194 pH is used preferentially as dilution tracer rather than temperature because it was measured
195 directly in the samples whereas temperature was derived from sensor data.

196 The total dissolved copper concentrations (TDCu) vary between 0.03 and 5.15 μM in the
197 samples (n = 42). These values are clearly far greater (one to three orders of magnitude) than
198 the ones reported for deep North Atlantic waters, i.e. 1.0 to 3.2 nM (Bruland and Franks,
199 1983; Donat and Bruland, 1995; Saager et al., 1997; Le Gall et al., 1999), indicating a marked
200 copper enrichment due to hydrothermal inputs. These concentrations are also lower than the
201 20-34 μM of total copper estimated by Von Damm et al. (1998), Charlou et al. (2000) and
202 Douville et al. (2002) in the Tour Eiffel endmember fluid. Our copper concentrations fall
203 within the range of the ones reported for the same area or for other hydrothermal systems
204 colonized by vent fauna (Table 2) and they are in accordance with the ones previously
205 reported by Geret et al. (1998) for the Tour Eiffel site. Surprisingly, the ranges are
206 comparable to the concentrations found in other hydrothermal systems characterized by
207 different geographical (EPR and MAR) and geological settings (Rainbow and Lucky Strike)

208 with likely differences in the chemical composition and the biogeochemistry of the mixing
209 zones. However, the concentrations previously published represent the concentration found in
210 unfiltered samples. Finally, the variability observed is important with concentrations of total
211 dissolved copper spreading between 0.03 to 5.15 μM in a 17°C temperature and 2 pH units
212 gradient.

213

214 *3.2 Dissolved copper species concentrations*

215 Inorganic and hydrophilic organic copper concentrations (non C_{18}Cu) range between 0.020
216 and 4.85 μM whereas hydrophobic organic copper levels (C_{18}Cu) vary from 0.001 to
217 0.095 μM . Thus, copper on the Tour Eiffel edifice occurs mainly as inorganic or hydrophilic
218 organic species whereas the C_{18}Cu fraction appears to be very low. This fraction, which was
219 measured for the first time in a hydrothermal environment, accounts only for $2 \pm 1\%$ of the
220 total dissolved copper ($n = 42$).

221 Compared to other marine environments, lower ratios of $\text{C}_{18}\text{Cu}/\text{TDCu}$ are obtained in this
222 hydrothermal system. As examples, in the North Atlantic and the North Pacific oceans,
223 hydrophobic organic complexes may represent 11 to 36% of the total dissolved copper
224 (Hanson and Quinn, 1983; Donat et al., 1986- filtration on 0.3 μm). In Mediterranean waters
225 filtered on 0.4 μm , the $\text{C}_{18}\text{Cu}/\text{TDCu}$ ratios were in the range of 11 to 55% (Elbaz-Poulichet et
226 al., 1994; Yoon et al., 1999). Studies conducted in estuarine systems and coastal waters report
227 slightly higher ratios compared to oceanic waters with values ranging from 11 to 66%
228 (Waeles et al., 2004- filtration on 0.45 μm).

229 The particularly low ratios obtained for our study may ensue from two complementary causes
230 or origins. Firstly, our experiments were conducted with endcapped C_{18} columns whereas the
231 previously cited studies used non-endcapped ones (Hanson and Quinn, 1983; Donat et al.,
232 1986; Elbaz-Poulichet et al., 1994; Yoon et al., 1999). The latter type of columns is

233 susceptible to retain the non-polar hydrophobic forms, but also a part of the polar compounds
234 as well. The overestimation of the non-polar hydrophobic fraction by non-encapped columns
235 has been assessed on a coastal seawater sample prior to this study and has been also evaluated
236 by El Sayed and Aminot (2000) on samples of Mediterranean water. From our measurements,
237 the C₁₈ fraction retained by non-encapped columns ($52 \pm 7\%$) is twice higher than the one
238 retained by encapped columns ($26 \pm 5\%$). By using a Chelex-100 resin pre-treatment before
239 the C₁₈ extraction, El Sayed and Aminot (2000) found a C₁₈Cu/TDCu ratio of $6.6 \pm 0.4\%$
240 whereas a 3-fold ratio ($21.8 \pm 1.7\%$) was reported after extraction when using only the non-
241 encapped C₁₈ columns.

242 Secondly, the low hydrophobic organic copper complexation observed in hydrothermal
243 waters can be cross-checked with the results of Sander et al. (2007). Over their study on three
244 different vent fields, they found that 11% of copper or more should be complexed by organic
245 matter. By comparison, estimations in estuarine and coastal media indicated that more than
246 99% of copper is organically complexed (Donat et al., 1994). Organic ligands can have
247 different origins in the hydrothermal environment studied. For example, Holms and Charlou,
248 (2001) observed the abiotic production of linear saturated hydrocarbons (C₁₆-C₂₉) during the
249 hydrothermal process in ultramafic systems. A potentially important source will be the
250 complex detritic organic matter produced by hydrothermal faunal assemblages (Limen et al.,
251 2001). Finally, the production of microbial exopolysaccharides have been revealed in deep
252 sea vents (Nichols et al., 2005). These extracellular polymers have been shown to possess
253 strong metal chelating properties (Loaec et al. 1998). Indeed, in hydrothermal systems,
254 sulphides which form stable complexes with copper [$K'(\text{CuL}) = 11.5$ (Al-Farawati and van
255 den Berg, 1999)] may be present at concentrations 250-fold higher than that of copper organic
256 ligands. Such high sulphide levels should limit the formation of organic complexes and
257 particularly of non-polar hydrophobic ones even though other metals such as Fe or Zn, which

258 have higher concentrations than Cu in hydrothermal fluids, can also compete for sulphide as
259 potential ligands. Al-Farawati and van den Berg (1999) determined the stability constant of
260 metal sulphides complexes in pH 8 seawater. In the presence of organic ligands, the copper
261 organic species are dominant for sulphide < 1 nM (i.e. Cu < sulphide). At higher levels of
262 sulphide, copper monobisulphide (CuHS^+) and copper dibisulphide [$\text{Cu}(\text{HS})_2$] will constitute
263 the major species. In this study, the total sulphide concentration was measured in situ and
264 ranges between 0.1 to 69 μM . The resulting ratio $\text{H}_2\text{S}_\text{T}/\text{TDCu}$ varies from 1.8 at pH 7 to 400
265 at pH 5.7 ($\text{H}_2\text{S}_\text{T} = 40 \mu\text{M}$, $\text{TDCu} = 0.1 \mu\text{M}$). The measured values are always in the case of a
266 $\text{H}_2\text{S}_\text{T}/\text{Cu} > 1$ favouring the formation of inorganic sulphide complex (copper mono bisulphide
267 and copper dibisulphide) rather than organic complexes according to the laboratory work
268 done by Al-Farawati and van den Berg (1999).

269

270 *3.3 Copper behaviour in the hydrothermal fluid-seawater mixing zone*

271 Figure 4 depicts the variations of TDCu, C_{18}Cu and $\text{nonC}_{18}\text{Cu}$ concentrations versus pH. The
272 pH decrease indicates an increase of the hydrothermal input. TDCu levels increase from 33 to
273 approximately 1000 nM for a pH varying between 5.6 and 6.5 and then reach a plateau (1310
274 ± 690 nM; $n = 30$) for higher pH values. The C_{18}Cu and $\text{nonC}_{18}\text{Cu}$ forms follow the same
275 trend than TDCu as expected from section 3.2. In the pH range of 5.6 - 6.5, these fractions
276 increase from 1 to approximately 20 nM and from 20 to approximately 1000 nM,
277 respectively. At pH > 6.5, their concentrations are relatively constant; i.e. 22 ± 18 nM and
278 1250 ± 680 nM, respectively. It is worth noting that the various copper fractions in the
279 hydrothermal fluid-richest sampled waters that were collected in a diffuse venting area (boxed
280 area in Figure 4) show higher levels than those observed at pH 5.6 and collected within a
281 mussel clumps.

282 In this part of the mixing zone, copper does not follow a conservative behaviour since it does
283 not show any negative correlation with pH. Theoretical copper concentrations following a
284 simple dilution process were estimated using the data published by Charlou et al. (2000). Our
285 data fall well above this theoretical mixing line for $\text{pH} > 6$, and are close or below this line for
286 $\text{pH} < 6$ (Figure 4, dotted line).

287 In order to explain the peculiar behaviour of copper in this part of the mixing zone, the
288 fluctuations of dissolved oxygen (O_2) and total sulphide (ΣS) in the studied area are also
289 presented (Figure 5 and 6). Dissolved oxygen was measured in situ with an Aanderaa optode
290 moored in a neighbouring mussel clump. The results obtained show an expected decrease in
291 oxygen concentration when increasing the hydrothermal input of reduced species. Total
292 sulphide was measured in situ at the 12 sampling points with the chemical analyzer
293 CHEMINI. The total sulphide vs. pH curve presents an inflexion point between pH 6.5 and 7.
294 The data clearly highlight the presence of a transition area at a pH around 6.7 between high
295 sulphide/low oxygen waters and low sulphide/high oxygen waters. It can be seen that the
296 lowest Cu concentrations measured at $\text{pH} < 6$ (Figure 4) correspond to high sulphide/low
297 oxygen area. In this acidic part of the mixing zone, the copper concentration might be
298 controlled by precipitation with sulphide. As a matter of fact, James and Elderfield (1996)
299 observed in the Snake pit vent field (MAR) that only 43% of copper was present in the
300 dissolved fraction ($< 0.4 \mu\text{M}$). Copper occurs mainly as sulphides (such as chalcopyrite) that
301 form large sized grains and settle rapidly in the near field region (Trocine and Trefy, 1988;
302 Feely et al., 1994).

303 For $\text{pH} > 6$, the dissolved Cu concentrations follow a trend opposite to a conservative
304 behaviour: TDCu concentrations increase to reach a plateau at pH around 6.5. In the same pH
305 range, total sulphide levels are characterized by a sharp drop from 40 to ca. $10 \mu\text{M}$. In the pH
306 range 6 - 6.5, the copper enrichment observed could be related to the dissolution of settled

307 copper sulphide particles in the presence of dissolved oxygen. The speciation of dissolved
308 copper obtained in this study supports this hypothesis as most of the dissolved copper (>
309 96%) is present under inorganic or hydrophilic organic complexes. Such an oxidative
310 redissolution (oxic alteration) phenomenon has already been advanced to explain the
311 variations of dissolved copper in hydrothermal fluids during the oxidation of chalcopyrite by
312 seawater or diluted fluids (Metz and Trefry, 2000). In hydrothermal sediments from the EPR,
313 Cu is associated to Fe oxyhydroxides that can undergo dissolution under oxic conditions and
314 finally precipitate as goethite (Dunk and Mills, 2006). In the sediments of the TAG
315 hydrothermal field (26°N, MAR), Severmann et al. (2006) reported elevated dissolved Cu
316 concentrations (< 0.2 μM) that might be caused by reaction between hydrothermal minerals
317 with oxygenated seawater within the suboxic/oxic area and producing a remobilization of Cu.
318 Oxidative redissolution processes were also observed in other marine systems. For example,
319 Paucot and Wollast (1997) reported in the Scheldt estuary a removal of dissolved Cu (< 0.45
320 μM) at low salinities due to sulphide precipitation in the anoxic part of the system. At higher
321 salinities and higher oxygen content, an increase of the dissolved fraction occurred as the
322 result of the redissolution of sulphide in oxic conditions.

323 For pH values higher than 7.5, one should expect in our system a strong decrease of dissolved
324 copper to reach the typical concentrations values of deep seawater (i.e. in the range 1-3 nM).

325 In Figure 7, we propose a conceptual model forecasting the copper behaviour over the entire
326 hydrothermal fluid-seawater mixing zone. Three major phenomenon should be considered: (i)
327 the precipitation of copper with hydrogen sulphide in the anoxic area close to the vent orifice
328 at pH < 6; (ii) the oxidative redissolution of accumulated copper sulphides particles to form
329 inorganic and hydrophilic organic complexes with increasing oxygen concentrations for pH
330 between 6 and 7.5 and (iii) the dilution of high metal content waters with low Cu seawater.

331

332 *3.4 Ecological significance*

333 The observed remobilisation of dissolved copper in the part of the mixing zone that
334 corresponds to the preferred habitat of *Bathymodiolus azoricus* faunal assemblages can have
335 an important biological significance. This mytilid mussel is the dominant “engineering”
336 species colonizing the Tour Eiffel edifice (Desbruyères et al., 2001). This species hosts a dual
337 symbiotic population in its gills composed of methanotroph and sulfoxidant microorganisms
338 (Fiala-Medioni et al., 2002; Duperron et al., 2006). The morphology of its intestine suggests
339 also a residual dependence on filter feeding (Fiala-Medioni et al., 2002). Metals like Fe, Zn
340 and Cu are essential for live organisms but may become toxic if present in excess.
341 Bioaccumulation in *B. azoricus* from the MAR occurs mainly in the gills that correspond to
342 the main interface between the organism and its environment and also in the digestive gland
343 (Cosson et al., 2008). Furthermore, metal bioaccumulation appears to be related to the
344 specificity of each vent field and reflects partly the chemical composition of the hydrothermal
345 fluid (Cosson et al., 2008). Even though the main bioaccumulation pathway of metals in
346 bivalves comes from their trophic uptake (Wang, 2002; Wang and Rainbow, 2005), it was
347 shown that they can directly intake the metals from the solute phase through permeable
348 surfaces including the gills (Marsden and Rainbow, 2004). This pathway will be strongly
349 influenced by the speciation of dissolved metals, including the hydrophilic / hydrophobic
350 properties of metallic complexes. Metals in solution may be taken up across permeable
351 membranes via different transport routes. A metal ion can either bind with a carrier protein
352 that mediate the transport through the membrane or it can cross the membrane using ionic
353 channels formed by a protein with a hydrophilic core. In addition, some hydrophobic
354 complexes can cross directly the bilayer lipidic cell membrane and can be released in the
355 cytoplasm. Nevertheless, this entry route appears to be quite limited (Simkiss, 1998). In
356 summary, the main intake processes of dissolved metals involve ionic channels and are

357 directly linked to the concentration of labile metal species (Simkiss, 1998). Therefore, the
358 presence of a secondary source of dissolved copper, associated with the accumulation of
359 metal sulphide particles, could play a significant role in the distribution of fauna in the
360 different habitats available at vents. Whether different hydrothermal fauna have different
361 tolerance and/or adaptation to deal with copper concentrations remains to be investigated.

362

363 **4. Conclusion**

364 In this study focused on the Tour Eiffel edifice (Lucky Strike vent field, MAR), levels of total
365 dissolved copper range from 0.03 μM to 5.15 μM . These values are much higher than the
366 ones reported for deep-sea oceanic waters but are in accordance with the ones previously
367 obtained in this area. Our data from speciation measurements show, for the first time, that the
368 hydrophobic organic fraction of copper (C_{18}Cu) is very low ($2 \pm 1\%$) in the hydrothermal
369 fluid-seawater mixing zone. On the other hand, copper is found mainly as inorganic and
370 hydrophilic organic complexes ($\text{nonC}_{18}\text{Cu}$). This result is especially interesting because this
371 latter fraction is liable to be more bioavailable than the former one. The distribution of copper
372 along the pH gradient shows the same pattern of evolution for each fraction. These fractions
373 highly increase from pH 5.6 to pH 6.5, then remain relatively constant at pH > 6.5. Oxygen
374 and sulphides data demonstrate that the copper anomaly at pH 6.5 is found in the transition
375 area between suboxic and oxic waters. Thus, the increase of dissolved copper should
376 correspond to the oxidative redissolution of copper sulphide particles formed in the vicinity of
377 the fluid exit. Moreover, our data indicate that the inorganic and hydrophilic organic fraction
378 is the one to be mainly affected by this oxidative redissolution mechanism.

379 Further work will be done on the whole mixing zone from the hot or diffuse emission to the
380 seawater pole to check the proposed behaviour. In addition, the data acquired during this

381 study will be used to look at the relationship between chemical gradients and species
382 distribution within *Bathymodiolus azoricus* mussel assemblages,

383

384 Acknowledgements

385 We would like to thank Captain Philippe Guillemet of the R/V “Pourquoi pas?” and his crew
386 for their never-failing collaboration in the success of the MoMARETO cruise. We also
387 acknowledge the Victor 6000 ROV pilots for their patience and constant support. This work
388 was done with the financial support of the European Union EXOCET/D project (FP6-GOCE-
389 CT-2003-505342), the ANR Deep Oases (ANR06 BDV005) and the GDR ECCHIS.

390

391 **References**

- 392 Al-Farawati R, van den Berg CMG. Metal-sulfide complexation in seawater. *Marine*
393 *Chemistry* 1999; 63: 331.
- 394 Bebianno MJ, Company R, Serafim A, Camus L, Cosson RP, Fiala-Médoni A. Antioxidant
395 systems and lipid peroxidation in *Bathymodiolus azoricus* from Mid-Atlantic Ridge
396 hydrothermal vent fields. *Aquatic Toxicology* 2005; 75: 354.
- 397 Bruland KW, Franks RP. Mn, Ni, Cu, Zn and Cd in the Western North Atlantic. In: NATO
398 Conference series editor. Trace metals in seawater. 9. Plenum Press, NY, 1983, pp. 395.
- 399 Charlou JL, Donval JP, Douville E, Jean-Baptiste P, Radford-Knoery J, Fouquet Y, Dapoigny
400 A, Stievenard M. Compared geochemical signatures and the evolution of Menez Gwen
401 (37°50'N) and Lucky Strike (37°17'N) hydrothermal fluids, south of the Azores Triple
402 Junction on the Mid-Atlantic Ridge. *Chemical Geology* 2000; 171: 49.
- 403 Childress JJ, Fisher CR. The biology of hydrothermal vent animals: physiology, biochemistry
404 and autotrophic symbioses. In: Barnes M, A.D. Ansell, Gibson RN, editors.
405 *Oceanography and Marine Biology Annual Review*. 30. UCL press, 1992, pp. 337-441.
- 406 Cosson RP, Vivier JP. Interactions of metallic elements and organisms within hydrothermal
407 vents. *Cahiers de Biologie Marine* 1997; 38: 43-50.
- 408 Cosson RP, Thiébaud É, Company R, Castrec-Rouelle M, Colaço A, Martins I, Sarradin P-M,
409 Bebianno MJ. Spatial variation of metal bioaccumulation in the hydrothermal vent
410 mussel *Bathymodiolus azoricus*. *Marine Environmental Research* 2008; 65: 405.

411 Desbruyères D, Chevalloné P, Alayse AM, Jollivet D, Lallier FH, Jouin-Toulmond C, Zal F,
412 Sarradin PM, Cosson R, Caprais JC, Arndt C, O'Brien J, Guezennec J, Hourdez S, Riso
413 R, Gaill F, Laubier L, Toulmond A. Biology and ecology of the "Pompeii worm"
414 (*Alvinella pompejana* Desbruyères and Laubier), a normal dweller of an extreme deep-
415 sea environment: A synthesis of current knowledge and recent developments. Deep Sea
416 Research Part II: Topical Studies in Oceanography 1998; 45: 383.

417 Desbruyères D, Biscoito M, Caprais JC, Colaço A, Comtet T, Crassous P, Fouquet Y,
418 Khripounoff A, Le Bris N, Olu K, Riso R, Sarradin PM, Segonzac M, Vangriesheim A.
419 Variations in deep-sea hydrothermal vent communities on the Mid-Atlantic Ridge near
420 the Azores plateau. Deep Sea Research Part I: Oceanographic Research Papers 2001;
421 48: 1325.

422 Di Meo-Savoie CA, Luther GW, Cary SC. Physicochemical characterization of the
423 microhabitat of the epibionts associated with *Alvinella pompejana*, a hydrothermal vent
424 annelid. Geochimica et Cosmochimica Acta 2004; 68: 2055-2066.

425 Donat JR, Statham PJ, Bruland KW. An evaluation of a C-18 solid phase extraction technique
426 for isolating metal-organic complexes from central North Pacific Ocean waters. Marine
427 Chemistry 1986; 18: 85.

428 Donat JR, Lao KA, Bruland KW. Speciation of dissolved copper and nickel in South San
429 Francisco Bay: a multi method approach. Analytica Chimica Acta 1994; 284: 547-571.

430 Donat JR, Bruland KW. Trace metals in the oceans. In: Steinnes E, Salbu B, editors. Trace
431 elements in natural waters. CRC press, Boca Raton, FLA, USA, 1995, pp. 302.

432 Douville E, Charlou JL, Oelkers EH, Bienvenu P, Jove Colon CF, Donval JP, Fouquet Y,
433 Prieur D, Appriou P. The Rainbow vent fluids (36°14'N, MAR): the influence of
434 ultramafic rocks and phase separation on trace metal content in Mid-Atlantic Ridge
435 hydrothermal fluids. Chemical Geology 2002; 184: 37.

436 Dunk RM, Mills RA. The impact of oxic alteration on plume-derived transition metals in
437 ridge flank sediments from the East Pacific Rise. Marine Geology 2006; 229: 133.

438 Duperron S, Bergin C, Zielinski F, Blazejak A, Pernthaler A, McKiness ZP, DeChaine E,
439 Cavanaugh CM, Dubilier N. A dual symbiosis shared by two mussel species,
440 *Bathymodiolus azoricus* and *Bathymodiolus puteoserpentis* (Bivalvia: Mytilidae), from
441 hydrothermal vents along the northern Mid-Atlantic Ridge. Environmental
442 Microbiology 2006; 8: 1441-1447.

443 El Sayed MA, Aminot A. C₁₈ Sep-Pak Extractable Dissolved Organic Copper Related to
444 Hydrochemistry in the North-west Mediterranean. *Estuarine, Coastal and Shelf Science*
445 2000; 50: 835.

446 Elbaz-Poulichet F, Cauwet G, Guan DM, Faguet D, Barlow R, Mantoura RFC. C₁₈ Sep-Pak
447 extractable trace metals in waters from the Gulf of Lions. *Marine Chemistry* 1994; 46:
448 67.

449 Feely RA, Geiselman TL, Baker ET, Massoth GJ, Hammond SR. Distribution and
450 composition of hydrothermal plumes particles from the ASHES vent field at axial
451 volcano, Juan de Fuca ridge. *Journal of Geophysical Research* 1990; 95: 12855-12873.

452 Feely RA, Gendron JF, Baker ET, Lebon GT. Hydrothermal plumes along the East Pacific
453 Rise, 8°40' to 11°50'N: Particle distribution and composition. *Earth and Planetary*
454 *Science Letters* 1994; 128: 19.

455 Fiala-Medioni A, McKiness ZP, Dando P, Boulegue J, Mariotti A, Alayse-Danet AM,
456 Robinson JJ, Cavanaugh CM. Ultrastructural, biochemical, and immunological
457 characterization of two populations of the mytilid mussel *Bathymodiolus azoricus* from
458 the Mid-Atlantic Ridge: evidence for a dual symbiosis. *Marine Biology* 2002; 141:
459 1035-1043.

460 Fouquet Y, Ondreas H, Charlou JL, Donval JP, Radford-Knoery J, Costa I, Lourenco N,
461 Tivey MK. Atlantic lava lakes and hot vents. *Nature* 1995; 377: 201.

462 Geret F, Rouse N, Riso R, Sarradin PM, Cosson R. Metal compartmentalization and
463 metallothionein isoforms in mussels from the Mid-Atlantic Ridge; preliminary approach
464 to the fluid-organism relationship. *Cahiers de Biologie Marine* 1998; 39: 291-293.

465 Geret F, Riso R, Sarradin PM, Caprais JC, Cosson R. Metal bioaccumulation and storage
466 forms in the shrimp, *Rimicaris exoculata*, from the Rainbow hydrothermal field (Mid
467 Atlantic Ridge); preliminary approach to the fluid-organism relationship. *Cahiers de*
468 *Biologie Marine* 2002; 43: 43-52.

469 Hanson AK, Quinn JG. The distribution of dissolved and organically complexed copper and
470 nickel in the middle Atlantic Bight. *Canadian Journal of Fisheries and Aquatic Sciences*
471 1983; 40: 151-161.

472 Holm NG, Charlou JL. Initial indications of abiotic formation of hydrocarbons in the
473 Rainbow ultramafic hydrothermal system, Mid-Atlantic Ridge. *Earth and Planetary*
474 *Science Letters* 2001; 191: 1.

475 James RH, Elderfield H. Dissolved and particulate trace metals in hydrothermal plumes at the
476 Mid-Atlantic Ridge. *Geophysical Research Letters* 1996; 23: 3499-3502.

477 Kadar E, Costa V, Martins I, Santos RS, Powell JJ. Enrichment in Trace Metals (Al, Mn, Co,
478 Cu, Mo, Cd, Fe, Zn, Pb and Hg) of Macro-Invertebrate Habitats at Hydrothermal Vents
479 Along the Mid-Atlantic Ridge. *Hydrobiologia* 2005; 548: 191.

480 Le Bris N, Govenar B, Le Gall C, Fisher CR. Variability of physico-chemical conditions in
481 9°50'N EPR diffuse flow vent habitats. *Marine Chemistry* 2006; 98: 167.

482 Le Gall AC, Statham PJ, Morley NH, Hydes DJ, Hunt CH. Processes influencing distributions
483 and concentrations of Cd, Cu, Mn and Ni at the North West European shelf break.
484 *Marine Chemistry* 1999; 68: 97-115.

485 Limén H, Levesque C, Kim Juniper S. POM in macro-/meiofaunal food webs associated with
486 three flow regimes at deep-sea hydrothermal vents on Axial Volcano, Juan de Fuca
487 Ridge. *Marine Biology* 2007; 153: 129.

488 Loaïc M, Olier R, Guezennec J. Chelating properties of bacterial exopolysaccharides from
489 deep-sea hydrothermal vents. *Carbohydrate Polymers* 1998; 35: 65.

490 Luther GW, Rozan TF, Taillefert M, Nuzzio DB, Di Meo C, Shank TM, Lutz RA, Cary SC.
491 Chemical speciation drives hydrothermal vent ecology. *Nature* 2001; 410: 813-816.

492 Marsden ID, Rainbow PS. Does the accumulation of trace metals in crustaceans affect their
493 ecology- the amphipod example? *Journal of Experimental Marine Biology and Ecology*
494 2004; 300: 373.

495 Metz S, Trefry JH. Chemical and mineralogical influences on concentrations of trace metals
496 in hydrothermal fluids. *Geochimica et Cosmochimica Acta* 2000; 64: 2267.

497 Mills GL, Quinn JG. Isolation of dissolved organic matter and copper-organic complexes
498 from estuarine waters using reverse-phase liquid chromatography. *Marine Chemistry*
499 1981; 10: 93.

500 Nichols CAM, Guezennec J, Bowman JP. Bacterial Exopolysaccharides from Extreme
501 Marine Environments with Special Consideration of the Southern Ocean, Sea Ice, and
502 Deep-Sea Hydrothermal Vents: A Review. *Marine Biotechnology* 2005; 7: 253.

503 Paucot H, Wollast R. Transport and transformation of trace metals in the Scheldt estuary.
504 *Marine Chemistry* 1997; 58: 229.

505 Paulson AJ, Curl HC, Gendron JF. Partitioning of Cu in estuarine waters, I. Partitioning in a
506 poisoned system. *Marine Chemistry* 1994; 45: 67.

507 Riso RD, Le Corre P, Chaumery CJ. Rapid and simultaneous analysis of trace metals (Cu, Pb,
508 and Cd) in seawater by potentiometric stripping analysis. *Analytica Chimica Acta*
509 1997a; 351: 83-89.

510 Riso RD, Monbet P, Le Corre P. Measurement of copper in sea-water by constant current
511 stripping analysis (CCSA) with a rotating gold disk electrode. *The Analyst* 1997b; 122:
512 1593-1596.

513 Ruelas-Inzunza J, Soto LA, Paez-Osuna F. Heavy-metal accumulation in the hydrothermal
514 vent clam *Vesicomya gigas* from Guaymas basin, Gulf of California. *Deep Sea*
515 *Research I* 2003; 50: 757-761.

516 Ruelas-Inzunza J, Paez-Osuna F, Soto LA. Bioaccumulation of Cd, Co, Cr, Cu, Fe, Hg, Mn,
517 Ni, Pb and Zn in trophosome and vestimentum of the tube worm *Riftia pachyptila* from
518 Guaymas basin, Gulf of California. *Deep Sea Research Part I: Oceanographic Research*
519 *Papers* 2005; 52: 1319-1323.

520 Saager PM, de Baar HJW, de Jong JTM, Nolting RF, Schijf J. Hydrography and local sources
521 of dissolved trace metals Mn, Ni, Cu, and Cd in the northeast Atlantic Ocean. *Marine*
522 *Chemistry* 1997; 57: 195.

523 Sander SG, Koschinsky A, Massoth G, Stott M, Hunter KA. Organic complexation of copper
524 in deep-sea hydrothermal vent systems. *Environmental Chemistry* 2007; 4: 81-89.

525 Sarradin PM, Caprais JC, Riso R, Kerouel R, Aminot A. Chemical environment of the
526 hydrothermal mussel communities in the Lucky Strike and Menez Gwen vent fields,
527 MAR. *Cahiers de Biologie Marine* 1999; 40: 93-104.

528 Sarradin P-M, Sarrazin J, Allais AG, Almeida D, Brandou V, Boetius A, Buffier E, Coiras E,
529 Colaço A, Cormack A, Dentrecolas S, Desbruyères D, Dorval P, du Buf H, Dupont J,
530 Godfroy A, Gouillou M, Gronemann J, Hamel G, Hamon M, Hoge U, Lane D, Le Gall
531 C, Leroux D, Legrand J, Léon P, Lévêque JP, Masson M, Olu K, Pascoal A, Sauter E,
532 Sanfilippo L, Savino E, Sebastião L, Serrão Santos R, Shillito B, Siméoni P, Schultz A,
533 Sudreau JP, Taylor P, Vuillemin R, Waldmann C, Wenzhöfer F, Zal F. EXtreme
534 ecosystem studies in the deep OCEan: Technological Developments. *InterRidge News*
535 2007; 16: 17-21.

536 Sarradin P-M, Lannuzel D, Waeles M, Crassous P, Le Bris N, Caprais JC, Fouquet Y, Fabri
537 MC, Riso R. Dissolved and particulate metals (Fe, Zn, Cu, Cd, Pb) in two habitats from
538 an active hydrothermal field on the EPR at 13°N. *Science of The Total Environment*
539 2008; 392: 119-129.

540 Sarrazin J, Sarradin PM, and the cruise participants. MoMARETO: a cruise dedicated to the
541 spatio-temporal dynamics and the adaptations of hydrothermal vent fauna on the Mid-
542 Atlantic Ridge. *InterRidge News* 2006a; 15: 24-33.

543 Sarrazin J, Walter C, Sarradin PM, Brind'amour A, Desbruyères D, Briand P, Fabri MC, Van
544 Gaever S, Van Reusel A, Bachraty C, Thiébaud E. Community structure and
545 temperature dynamics within a mussel assemblage on the Southern East Pacific Rise.
546 Cahier de Biologie Marine 2006b; 47: 483-490.

547 Severmann S, Mills RA, Palmer MR, Telling JP, Cragg B, John Parkes R. The role of
548 prokaryotes in subsurface weathering of hydrothermal sediments: A combined
549 geochemical and microbiological investigation. Geochimica et Cosmochimica Acta
550 2006; 70: 1677.

551 Shillito B, Hamel G, Duchi C, Cottin D, Sarrazin J, Sarradin PM, Ravaux J, Gaill F. Live
552 capture of megafauna from 2300 m depth, using a newly designed Pressurized Recovery
553 Device. Deep Sea Research Part I: Oceanographic Research Papers; In Press.

554 Simkiss K. Mechanism of metal uptake. In: Langston WJ, Bebianno MJ, editors. Metal
555 metabolism in aquatic environments. Chapman & Hall Ltd, 1998, pp. 1-15.

556 Tengberg A, Hovdenes J, Andersson HJ, Brocandel O, Diaz R, Hebert D, Arnerich T, Huber
557 C, Körtzinger A, Khripounoff A, Rey F, Rønning C, Schimanski J, Sommer S,
558 Stangelmayer A. Evaluation of a lifetime-based optode to measure oxygen in aquatic
559 systems. Limnology and Oceanography: Methods 2006; 4: 7-17.

560 Trefry JH, Trocine RP. Iron and copper enrichment of suspended particles in dispersed
561 hydrothermal plumes along the Mid Atlantic Ridge. Geophysical Research Letters
562 1985; 12: 506-509.

563 Trocine RP, Trefry JH. Distribution and chemistry of suspended particles from an active
564 hydrothermal vent site on the Mid-Atlantic Ridge at 26°N. Earth and Planetary Science
565 Letters 1988; 88: 1-15.

566 Urcuyo IA, Massoth GJ, Julian D, Fisher CR. Habitat, growth and physiological ecology of a
567 basaltic community of *Ridgeia piscesae* from the Juan de Fuca Ridge. Deep Sea
568 Research Part I: Oceanographic Research Papers 2003; 50: 763.

569 Von Damm KL, Bray AM, Buttermore LG, Oosting SE. The geochemical controls on vent
570 fluids from the Lucky Strike vent field, Mid-Atlantic Ridge. Earth and Planetary
571 Science Letters 1998; 160: 521.

572 Vuillemin R, Le Roux D, Dorval P, Hamon M, Sudreau JP, Le Gall C, Sarradin PM.
573 CHEMINI: CHEMical MINIaturised analyzer: A new generation of in situ chemical
574 analyzers for marine applications. Instrumentation viewpoint 2007; 6: 9.

575 Vuillemin R, Le Roux D, Dorval P, Bucas K, Sudreau JP, Hamon M, Le Gall C, Sarradin PM.
576 CHEMINI: a new in situ CHEmical MINIaturized analyzer. Deep Sea Research part I
577 Instruments and methods submitted 06/2008.

578 Waeles M, Riso RD, Maguer J-F, Le Corre P. Distribution and chemical speciation of
579 dissolved cadmium and copper in the Loire estuary and North Biscay continental shelf,
580 France. Estuarine, Coastal and Shelf Science 2004; 59: 49.

581 Waeles M, Riso RD, Le Corre P. Seasonal variations of dissolved and particulate copper
582 species in estuarine waters. Estuarine, Coastal and Shelf Science 2005; 62: 313.

583 Wang W-X. Interactions of trace metals and different marine food chains. Marine Ecology
584 Progress Series 2002; 243: 295-309.

585 Wang W-X, Rainbow PS. Influence of metal exposure history on trace metal uptake and
586 accumulation by marine invertebrates. Ecotoxicology and Environmental Safety 2005;
587 61: 145.

588 Yoon Y-Y, Martin J-M, Cotté MH. Dissolved trace metals in the Western Mediterranean Sea:
589 total concentration and fraction isolated by C₁₈ Sep-Pak technique. Marine Chemistry
590 1999; 66: 129.

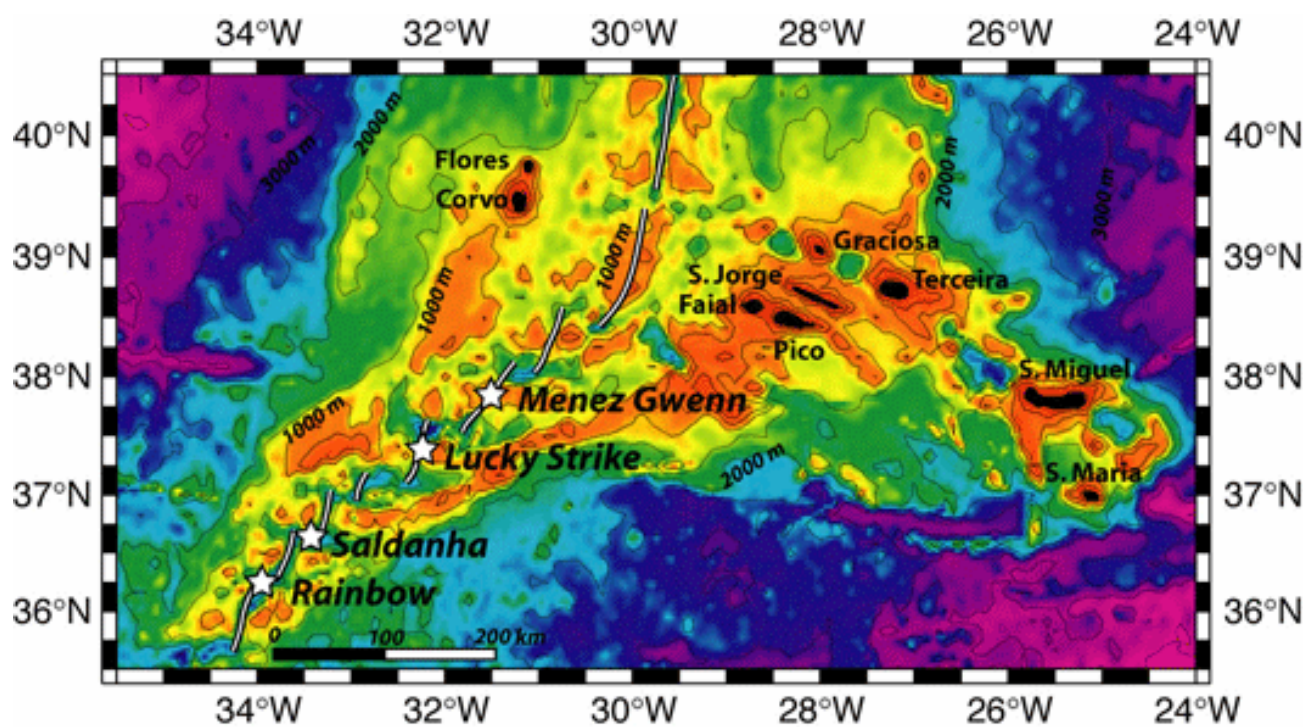


Fig. 1- Simplified bathymetric map of the Mid-Atlantic Ridge near the Azores (seafloor depths in meters), showing the location of the four main hydrothermal vent fields. (<http://www.momarfr.org/>)

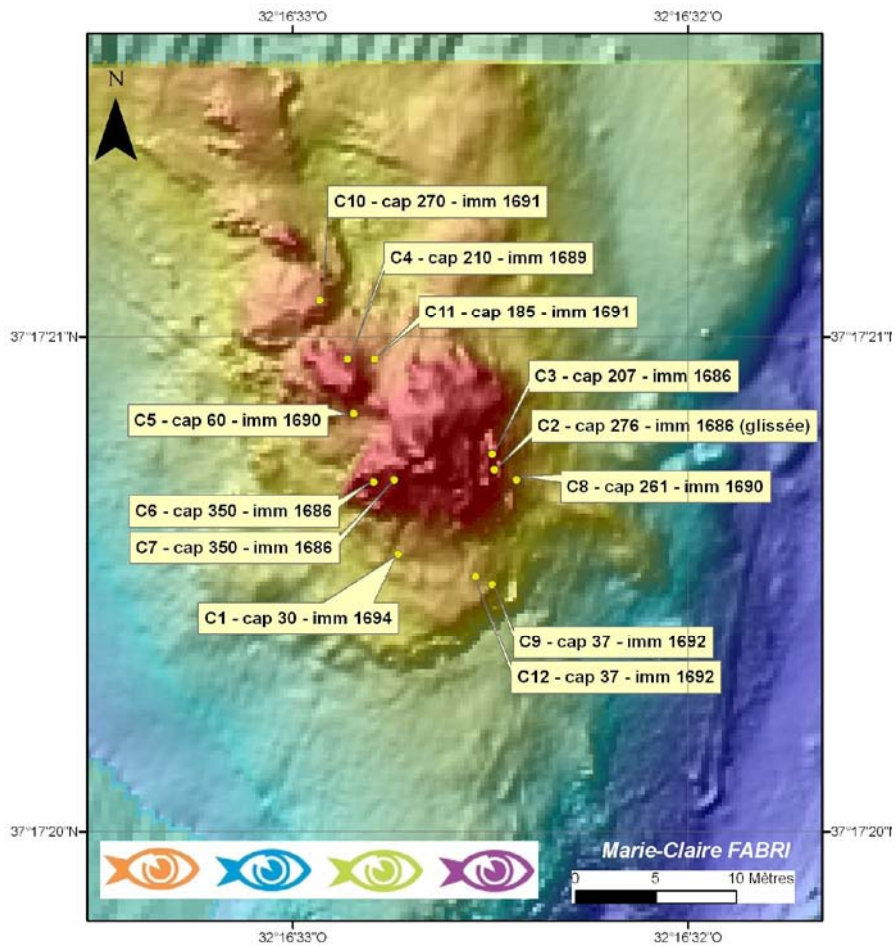


Fig. 2- Bathymetric map of the Tour Eiffel active edifice and location of the 12 sampling stations C1 to C12 (Sarrazin et al., 2006).

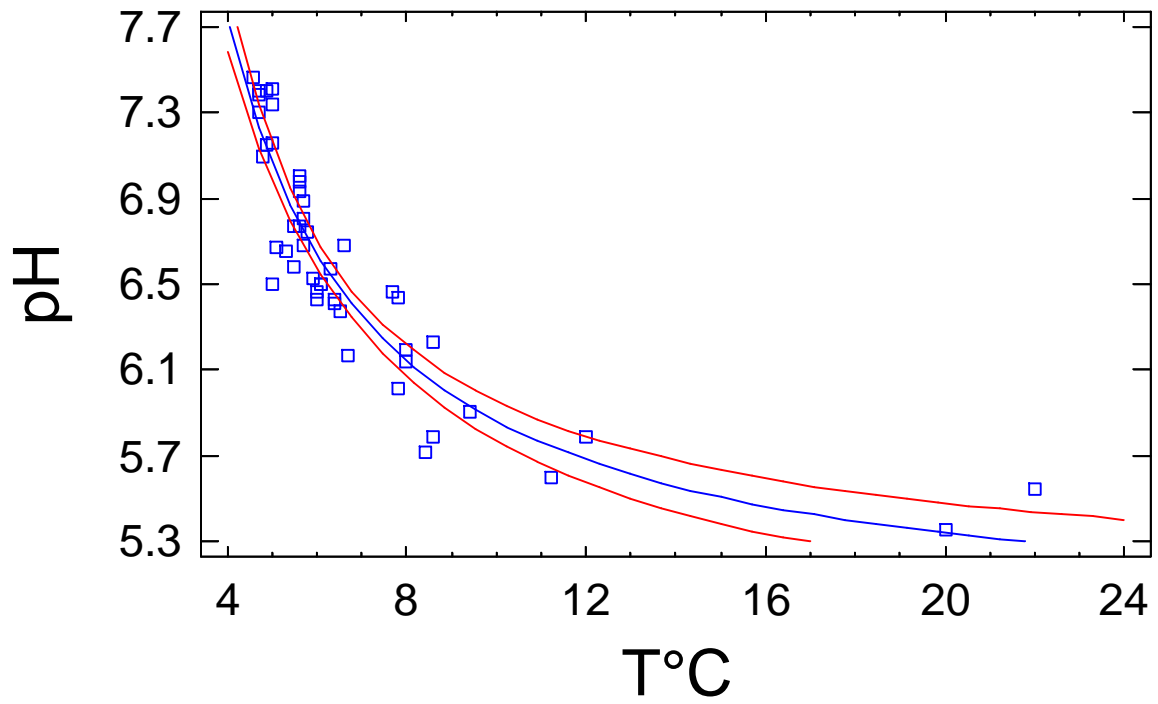


Fig. 3- Temperature/pH relationship obtained in the cold part of the mixing zone. $\text{pH}=\exp^{(1.582+1.857/T)}$, $R^2 = 86.6\%$, $n = 42$. The external lines represent the confidence interval at 95% (Statgraphics Plus).

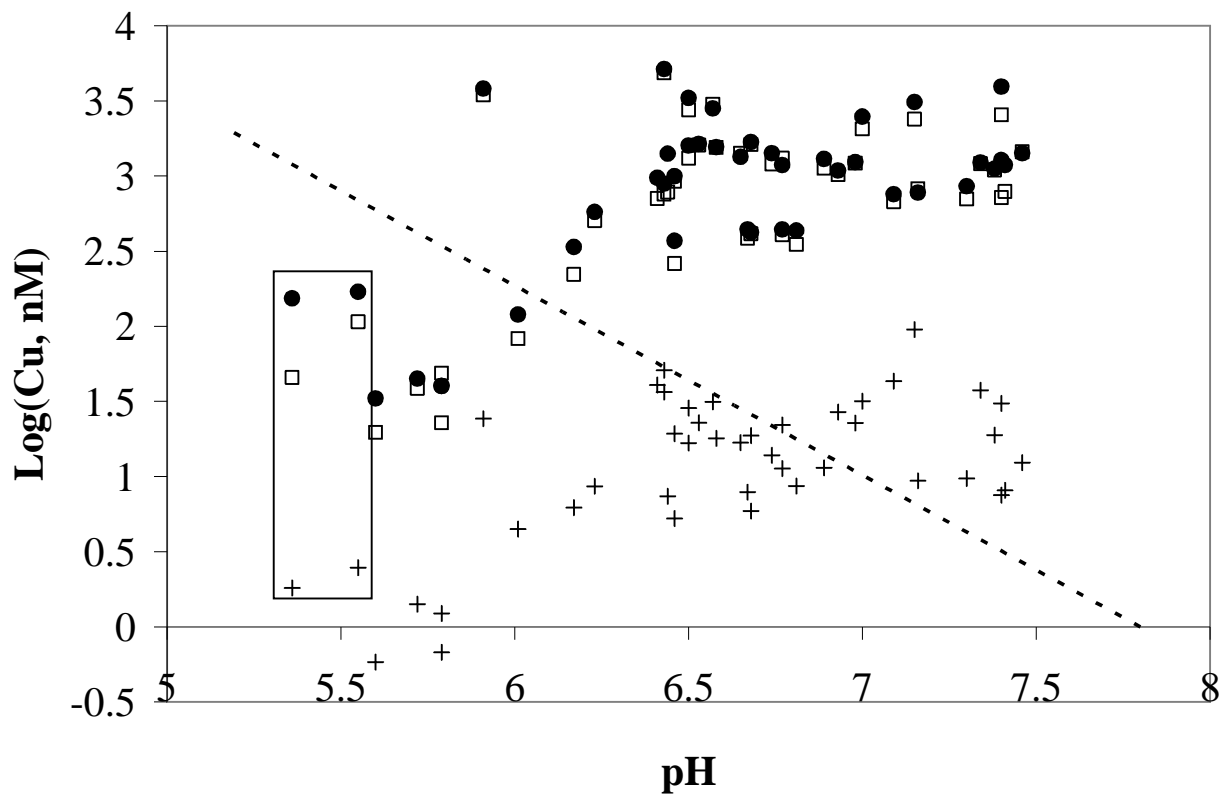


Fig. 4- Distribution of copper concentrations [Log (Cu, nM)] vs pH. TDCu (●), C₁₈Cu (+) nonC₁₈Cu (□). The boxed area indicates the samples with the lowest pH/highest temperature (~ 22°C) collected in a diffuse venting area. The dotted line represents a theoretical dilution of hydrothermal copper [pH = 4.3, Cu = 26000 nM, (Charlou et al., 2000)] by seawater, pH 7.8, Cu = 1 nM.

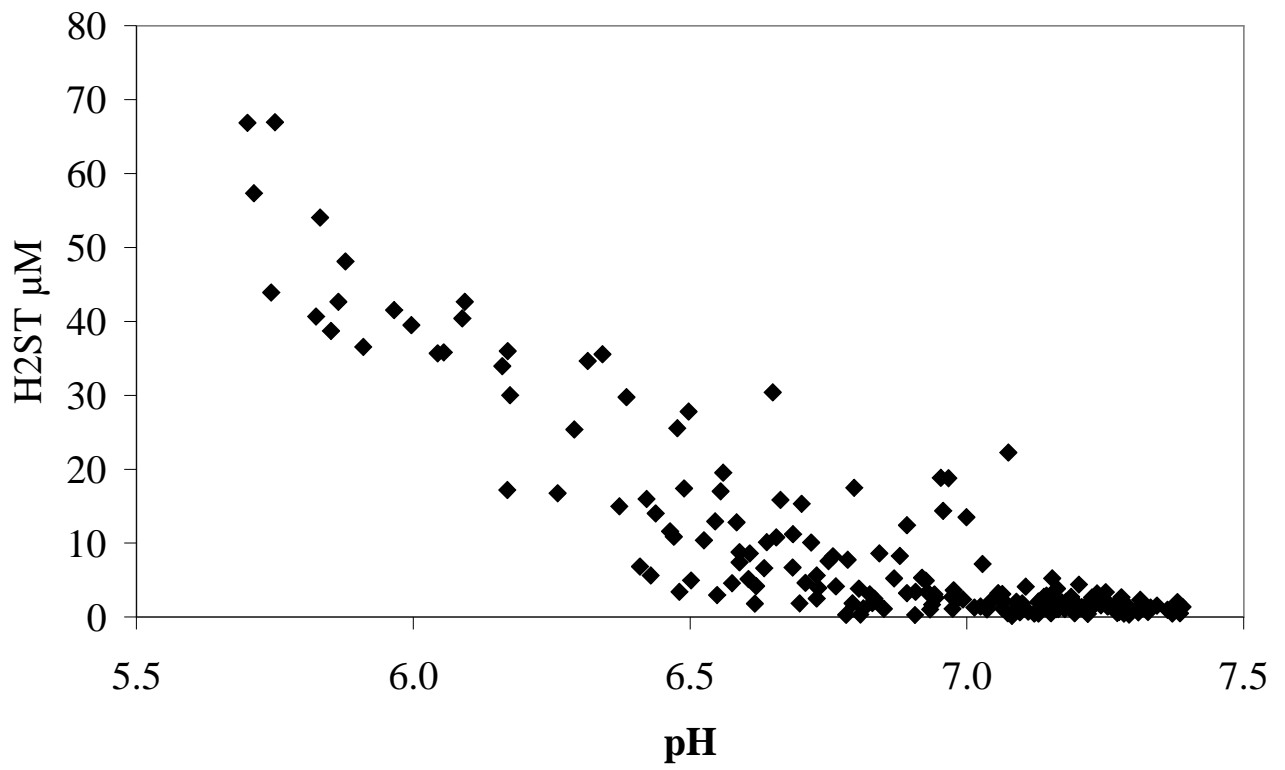


Fig. 5- Concentration of total sulphide measured in situ with the CHEMINI chemical analyzer on the 12 sampling points ($T = 4.5$ to 11.7°C , $n = 189$).

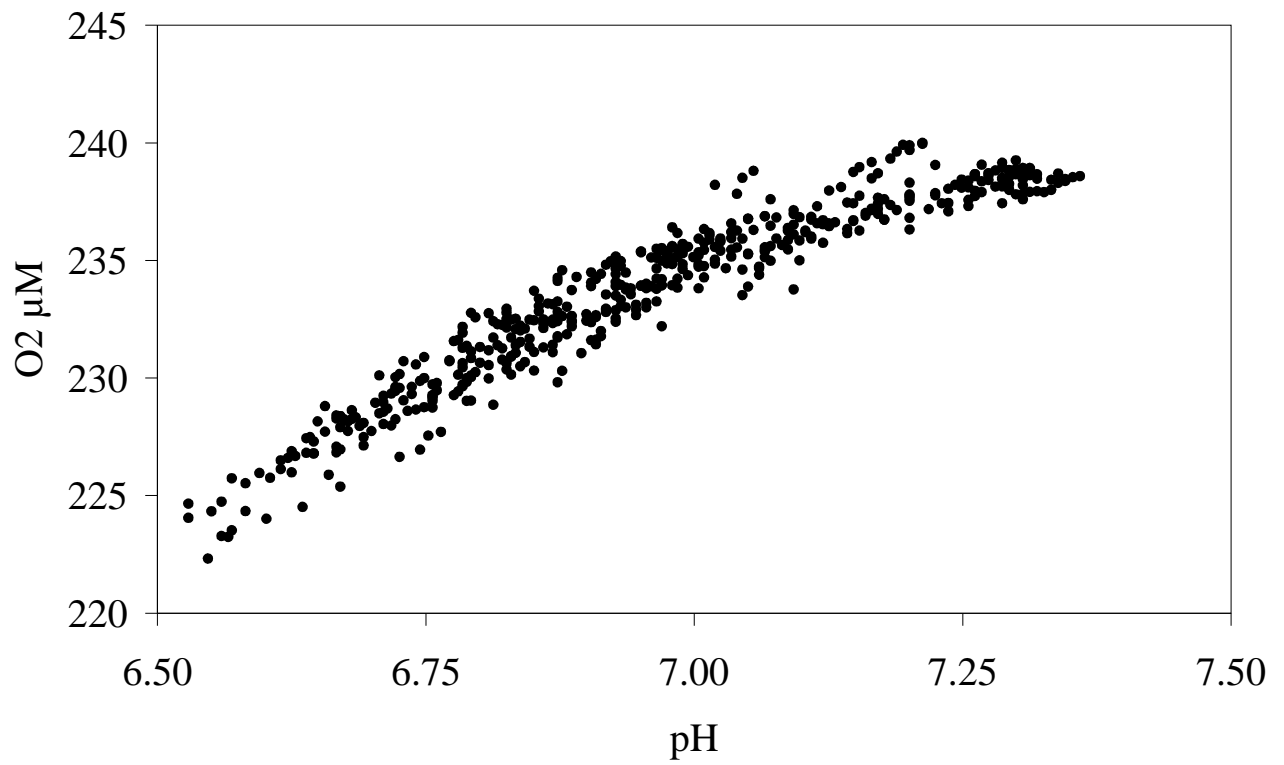


Fig. 6- Concentration of dissolved oxygen measured in situ by an Aanderaa optode in a neighbouring mussel clump during 4 hours (2 mes / min, n= 480, T = 4.5 to 6.3°C).

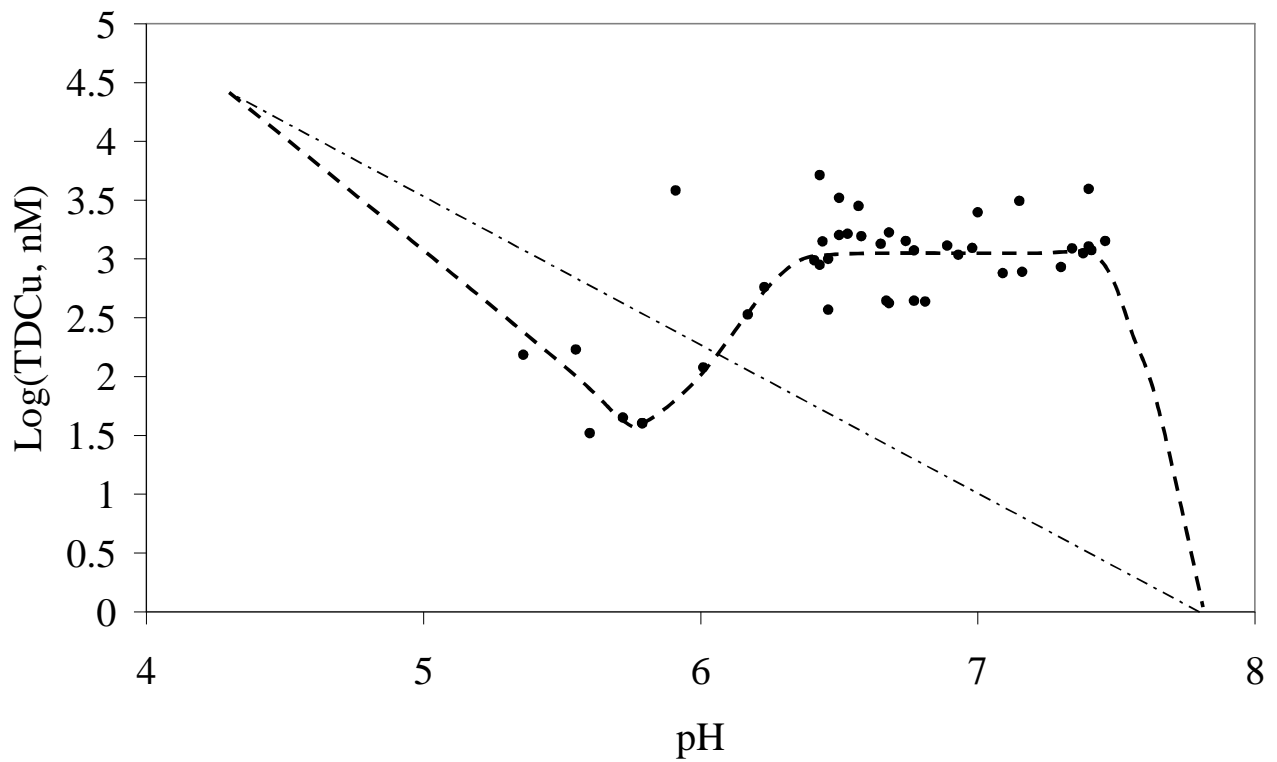


Fig. 7- Proposed schematic behaviour of dissolved copper in the hydrothermal fluid-seawater mixing zone. The dotted straight line represents the theoretical dilution of hydrothermal copper (pH = 4.3, T = 325, Cu = 26000 nM) by seawater.

TABLES

	Cu (nM)	
	Certified value	Measured value
NASS-5	4.7 ± 0.7	4.4 ± 0.2
CASS-3	8.1 ± 1.0	7.6 ± 0.5
SLEW-2	25.7 ± 1.7	27.2 ± 1.4

Table 1- Analysis of Cu in certified seawater samples: NASS-5 oceanic seawater, CASS-3 coastal seawater, SLEW-2 estuarine water. Values are expressed as mean \pm confidence interval (95%)

Hydrothermal fields	Cu (μM)	T$^{\circ}\text{C}$	pH	References
EPR, 9 $^{\circ}\text{N}$	0.08 - 2.10 ***	13 - 176	5.3 - 6.4	Di Meo-Savoie et al., 2004
EPR, 13 $^{\circ}\text{N}$	1.38 - 3.27*	-	5.7 - 7.5	Desbruyères et al., 1998
EPR, 13 $^{\circ}\text{N}$	0.18 - 1.6*	3.8 - 20	-	Sarradin et al., 2008
MAR, Rainbow	0.14 - 3.20*	4.7 - 25	6.3 - 7.5	Geret et al., 2002
MAR, LS, Tour Eiffel	0.02 - 2.05*	-	-	Geret et al., 1998
MAR, LS	1.13 **	4.3	6.2	Kadar et al., 2005
MAR, LS, Tour Eiffel	0.03 - 5.15 **	4.6 - 22	5.4 - 7.5	This study

Table 2- Concentrations of copper in various hydrothermal systems colonized by hydrothermal fauna. MAR: Mid Atlantic Ridge; EPR: East Pacific Rise; LS: Lucky Strike vent field. * unfiltered samples, ** samples filtered on a 0.45 μm filter. *** samples filtered and centrifugated.

Appendix 1 : pH, temperature and total dissolved copper obtained in the 43 samples.

pH measurements were performed onboard using a Metrohm® pH-meter with a combined pH electrode for sulphide rich medium. Sample temperatures were derived from the data recorded by the temperature probe associated with the sample inlet. Samples were filtered on board through a 0.45- μm -Millipore®-HATF filter. The separation and the quantification of the hydrophobic organic copper complexes (C_{18}Cu), and the inorganic and hydrophilic organic complexes ($\text{nonC}_{18}\text{Cu}$) were performed on shore.

Sample	pH	T°C	TDCu (μM)	nonC ₁₈ Cu (μM)	C ₁₈ Cu (μM)
296 A2	5.6	11.2	0.033	0.02	0.001
300 E1	5.72	8.4	0.045	0.04	0.001
300 D3	5.79	8.6	0.040	0.05	0.001
301 C1	5.79	12	0.040	0.02	0.001
300 D2	6.01	7.8	0.120	0.08	0.004
296 A1	6.17	6.7	0.337	0.22	0.006
297 A1	6.23	8.6	0.576	0.51	0.009
300 B2	6.41	6.4	0.976	0.71	0.041
296 B1	6.43	6	0.890	0.76	0.036
296 B2	6.43	6.4	5.151	4.85	0.051
301 C2	6.44	7.8	1.410	0.78	0.007
297 C1	6.46	7.7	1.00	0.92	0.019
300 B3	6.46	6	0.37	0.26	0.005
297 B2	6.5	5	3.31	2.76	0.029
300 C3	6.5	6.1	1.60	1.31	0.017
300 C1	6.53	5.9	1.64	1.61	0.023
301 B2	6.57	6.3	2.82	3.00	0.031
300 C2	6.58	5.5	1.56	1.55	0.018
301 B1	6.65	5.3	1.34	1.42	0.017
296 A3	6.67	5.11	0.44	0.39	0.008
297 B3	6.68	5.7	0.42	0.41	0.006
301 B3	6.68	6.6	1.68	1.62	0.019
301 A2	6.74	5.8	1.42	1.21	0.014
300 D1	6.77	5.6	1.18	1.31	0.022
300 B1	6.77	5.5	0.44	0.41	0.011
300 A3	6.81	5.7	0.43	0.35	0.009
297 B1	6.89	5.7	1.30	1.13	0.011
300 A1	6.93	5.6	1.09	1.02	0.027

300 A2	6.98	5.6	1.24	1.22	0.023
301 A1	7	5.6	2.49	2.06	0.032
297 E2	7.09	4.8	0.76	0.67	0.043
297 C3	7.15	4.9	3.11	2.40	0.095
301 A3	7.16	5	0.78	0.82	0.009
301 C3	7.3	4.7	0.86	0.70	0.010
297 D2	7.34	5	1.23	1.21	0.038
301 D1	7.38	4.7	1.12	1.10	0.019
297 D1	7.4	4.7	3.95	2.56	0.031
301 D2	7.4	4.9	1.28	0.72	0.008
301 D3	7.41	5	1.19	0.79	0.008
297 D3	7.46	4.6	1.42	1.45	0.012
297 C2	5.91	9.4	3.82	3.47	0.024
296 C1	5.55	22	0.17	0.11	0.002
296 B3	5.36	20	0.15	0.05	0.002
